



HHS Public Access

Author manuscript

IEEE/ACM Trans Comput Biol Bioinform. Author manuscript; available in PMC 2019 March 01.

Published in final edited form as:

IEEE/ACM Trans Comput Biol Bioinform. 2018 ; 15(2): 570–580. doi:10.1109/TCBB.2015.2465951.

Cortical Thinning and Cognitive Impairment in Parkinson's Disease Without Dementia

Lijun Zhang,

Institute for Personalized Medicine, Pennsylvania State University-College of Medicine, Hershey, PA 17033. lzhang6@hmc.psu.edu

Ming Wang,

Public Health Sciences, Pennsylvania State University-College of Medicine, Hershey, PA 17033. mwang@phs.psu.edu

Nicholas W. Sterling,

Dept of Neurology, Pennsylvania State University-Milton S. Hershey Medical Center, Hershey, PA 17033

Eun-Young Lee,

Dept of Neurology, Pennsylvania State University-Milton S. Hershey Medical Center, Hershey, PA 17033

Paul J. Eslinger,

Dept of Neurology, Public Health Sciences, and Radiology, Pennsylvania State University-Milton S. Hershey Medical Center, Hershey, PA 17033

Daymond Wagner,

Dept of Neurology, Pennsylvania State University-Milton S. Hershey Medical Center, Hershey, PA 17033

Guangwei Du,

Dept of Neurology, Pennsylvania State University-Milton S. Hershey Medical Center, Hershey, PA 17033

Mechelle M. Lewis,

Dept of Neurology, Pharmacology, Pennsylvania State University-Milton S. Hershey Medical Center, Hershey, PA 17033

Young Truong,

Dept of Biostatistics, University of North Carolina at Chapel Hill, NC, 27599

F. DuBois Bowman, and

Dept of Biostatistics, Columbia University, New York, NY 10032

Xuemei Huang

Personal use is permitted, but republication/redistribution requires IEEE permission. See http://www.ieee.org/publications_standards/publications/rights/index.html for more information.

Correspondence to: Xuemei Huang.

L. Zhang and M. Wang have equal contribution as cofirst authors

Dept of Neurology, Pharmacology, Radiology, Neurosurgery, and Kinesiology, Pennsylvania State University-Milton S. Hershey Medical Center, Hershey, PA 17033. xuemei@psu.edu

Abstract

Parkinson's disease (PD) is a progressive neurodegenerative disorder characterized clinically by motor dysfunction (bradykinesia, rigidity, tremor, and postural instability), and pathologically by the loss of dopaminergic neurons in the substantia nigra of basal ganglia. Growing literature supports that cognitive deficits may also be present in PD, even in non-demented patients. Gray matter (GM) atrophy has been reported in PD and may be related to cognitive decline. This study investigated cortical thickness in non-demented PD subjects and elucidated its relationships to cognitive impairment using High-resolution T1-weighted brain MRI and comprehensive cognitive function from 71 non-demented PD and 48 control subjects matched for age, gender, and education. Cortical thickness was compared between groups using a flexible hierarchical multivariate Bayesian model, which accounts for correlations between brain regions. Correlation analyses were performed among brain areas and cognitive domains as well, which showed significant group differences in the PD population. Compared to Controls, PD subjects demonstrated significant age-adjusted cortical thinning predominantly in inferior and superior parietal areas and extended to superior frontal, superior temporal, and precuneus areas (posterior probability > 0.9). Cortical thinning was also found in the left precentral and lateral occipital, and right postcentral, middle frontal, and fusiform regions (posterior probability > 0.9). PD patients showed significantly reduced cognitive performance in executive function, including set shifting ($p=0.005$) and spontaneous flexibility ($p=0.02$), which were associated with the above cortical thinning regions ($p < 0.05$).

Index Terms

Parkinson's Disease; Cognitive Impairment; MRI; Cortical Thickness; Hierarchical Bayesian Model

1 Introduction

Parkinson's disease (PD) is a progressive neurodegenerative disorder marked clinically by motor dysfunction and associates pathologically with the loss of dopaminergic neurons in the substantia nigra pars compacta (SNc) of the basal ganglia (BG). Many non-motor symptoms are also present in PD and often attributed to extranigral non-dopaminergic system dysfunction [1]. Despite many effective dopamine replacement treatments, PD patients experience progressively more motor and non-motor disabilities, including cognitive, sensory, and emotional impairments [2], [3], [4]. Long-term followup studies have shown that 83% of PD patients suffer from dementia within 20 years of diagnosis [5], [6], [7]. Braak et al. [8] have hypothesized that the progression of a diverse spectrum of motor and non-motor dysfunction is likely related to the ascending spread of α -synuclein-immunopositive Lewy bodies and neurites from lower brainstem nuclei to cortical gray areas. The cortical involvement of Lewy bodies in PD was postulated to initiate in the temporal mesocortex region (stage 4), continue to the prefrontal cortex (stage 5), and finally reach to the primary sensory and premotor areas (stage 6) [8]. Although it is still unclear

whether Lewy bodies are the direct cause of neuronal degeneration, the pathological changes in the cortex may relate directly to cognitive impairment in PD.

Several *in vivo* functional neuroimaging studies of PD patients have been used to assess the neurodegenerative progression and their functional correlations in PD. For example, positron emission tomography (PET) studies have attempted to define abnormal covariance patterns of cortical and subcortical regional glucose metabolism that correlated with cognitive impairment [9], [10]. fMRI studies revealed the relationship between cognitive impairments and reduced neural activity in frontostriatal circuitry [3]. These functional neurological assessments, however, may be influenced by symptomatic treatments and functional states of patients.

Structural volumetric measurements with high-resolution magnetic resonance imaging (MRI) may reflect *in vivo* macroscopic atrophy of the regions of interest (ROIs) and have been adopted to characterize the pathological process. Recent MRI studies using voxel-based morphometry (VBM) revealed a correlation of grey matter (GM) atrophy with disease stage and cognitive impairment in PD [11], [12], [13]. The results in nondemented PD were, however, more variable, with some studies reporting regional GM atrophy in frontal, temporal, or parietal cortex [14]. Conversely, some studies have shown no cortical atrophy in PD [15], [16]. The variability of VBM results and the lack of a consistent portrait of damage in the cerebral cortex may be due partly to non-specific spatial smoothing that mixes voxels far apart on the plane (e.g., on different hemispheres or sides of a sulcus) [17], [18].

Cortical thickness measures the shortest distances between a given brain surface and inner edge of cortical gray matter and may more directly reflect the underlying cyto- and myeloarchitecture of cortical structural changes. For example, it has been shown that neurons within the cerebral cortex are organized into ontogenetic columns that run perpendicular to the brain surface [19], and the cortical thickness measurement was linked to the number of cells within a column, reflecting the density of neuronal cell bodies and/or synaptic connections and the myelination of fibers [20], [21], [22] [23]. Thus, cortical thickness has been hypothesized to be a more promising tool to investigate GM changes related to PD cortical pathology. Consistent with this hypothesis, it has been demonstrated that cortical thinning occurs in both mild and advanced PD patients [24], [25], [26] [27], and can be associated with disease duration. In addition, accelerated cortical thickness changes and cognitive impairment have been reported in PD patients older than 70 years of age [28], [29] [30]. Studies in PD without dementia have reported cortical folding abnormalities and GM volume reductions [31]. However, it remains unclear whether there is any relationship with cognitive changes, and how cortical thickness is related to cognitive impairment in PD without dementia [32].

In this study, we tested the hypothesis that changes in cortical thinning can be detected in PD patients without dementia and these changes are correlated with measured cognitive decline. We adopted an advanced hierarchical multivariate Bayesian model to analyze the cortical thickness measurement and thinning pattern, which can take regions' dependence into account using high resolution MRI on a large cohort of relatively younger PD patients without evidences of dementia. The basic analytic framework for the Bayesian model has

been previously applied to fMRI data [33], [34], and here we extend it for the first time for the analysis of cortical thickness. In addition, we performed correlation analysis between cortical thickness and neuropsychological tests to assess the neural substrates of cognitive decline in PD.

2 Materials and Methods

2.1 Participants

Patients with PD and control subjects (Control) were recruited for an ongoing study approved by the Institutional Review Board/Human Subjects Protection Office (IRB/HSPO) of Pennsylvania State Hershey Medical Center. All participants provided written informed consent in accordance with IRB/HSPO guidelines and the Declaration of Helsinki.

71 PD patients without dementia were included in this study, who were diagnosed by a movement disorders specialist according to the published criteria [35], and were optimally managed with anti-parkinsonian medications. 48 Controls matched with PD patients for age, gender, education, and handedness, were selected from a pool of controls that were part of the ongoing study. Controls were free from any history of neurologic or psychiatric disorder, including previous head injury. All subjects were negative for other neurological history, hypothyroidism, vitamin B12 and folate deficiencies, and kidney and liver disease. None of the PD or Controls were demented with MMSE > 25 and DRS-2 > 10 [36], [37].

For both motor and cognitive tests, PD patients were assessed in a practically defined “off” state after withholding all medications overnight (~12 hours) [38]. Unified Parkinson’s Disease Rating Scale III (UPDRS) scores were recorded for all subjects and verified by a second rater from video recordings of the original assessment, except the rigidity. Disease severity was also recorded using Hoehn and Yahr staging [39].

2.2 Cognitive Assessment

All subjects were administered a standardized neuropsychological battery, along with the Hamilton Depression Scale (HAM-D) [40]. Montreal Cognitive Assessment (MoCA) [41] and the Dementia Rating Scale, Second Edition (DRS-2) [36]. One fine motor function domain and six cognitive domains were examined [13]: (1) processing speed, (2) Executive functions [set-shifting and spontaneous flexibility], (3) language, (4) learning/memory, (5) spatial cognition, and (6) attention/working memory. Each domain was assessed by two or more tests, except for the fine motor speed [13].

2.2 Neuroimaging Data Acquisition and Preprocessing

MRIs were acquired on a Siemens 3-Tesla TimTrio equipped with an 8-channel birdcage type In vivo coil. High-resolution T1-weighted (T1W) MRI images (3D MPRAGE, TR=1540 ms, TE=2.3 ms, voxel spacing 1.0×1.0×1.0 mm, image resolution 256×256 mm², 176 slices with no gap) were acquired for cortical thickness analysis.

Cortical thickness data were obtained using the Free-Surfer software package (version 5.3, available at: <http://surfer.nmr.harvard.edu>). The automated procedures first include resampling T1W MR images, motion correction, removal of non-brain tissue via a hybrid

surface deformation procedure [42]; Second, automated Talairach transformation, segmentation of the subcortical white matter (WM) and deep GM volumetric structures were applied [43]; Third is intensity normalization [44]; And then, tessellation of the GM/WM boundary, automated topology correction [45], and surface deformation following intensity gradients to place optimally the GM/WM and GM/cerebrospinal fluid borders at the location where the greatest shift in intensity defines the transition to the other tissue class [46], [47]. Cortical thickness was measured at each vertex of the WM/GM boundary by computing the shortest distance toward the pial surface. Cortical thickness maps were smoothed using a Gaussian kernel across the surface with a FWHM of 10 mm and averaged across subjects.

3 Statistical Analyses

3.1 MRI Thickness Analysis

We adopted a flexible multivariate Bayesian approach, based on an in-house hierarchical Bayesian model that enables the user to formulate probabilistic statements to quantify the evidence for cortical thickness differences between PD and Controls (http://web1.sph.emory.edu/bios/CBIS/download_page.php). We extend the previous formulation of the model for fMRI data [33], [34] to analyze cortical thinning associated with PD. The hierarchical Bayesian model accounts for both spatial correlations between intra-regional voxels as well as between distinct cortical regions. Along the lines of Bowman et al. [33], the Bayesian model has the following hierarchical structure:

$$Y_{ij} | \mu_{gj}, \alpha_{ij}, x_{ijq}, \sigma_{gj}^2 \sim MVN(\mu_{gj} + \mathbf{1}\alpha_{ij} + \sum_{q=1}^Q \gamma_{gj} x_{ijq}, \sigma_{gj}^2 \mathbf{I})$$

$$\mu_{gj} | \lambda_{gj}^2 \sim MVN(\mathbf{1}\mu_{0gj}, \lambda_{gj}^2 \mathbf{I})$$

$$\gamma_{gj} | \tau_{gj}^2 \sim MVN(\mathbf{1}\gamma_{0gj}, \tau_{gj}^2 \mathbf{I})$$

$$\sigma_{gj}^2 \sim \text{Gamma}(a_0, b_0)$$

$$\alpha_{ij} \sim MVN(0, \Gamma_j)$$

$$\lambda_{gj}^2 \sim \text{Gamma}(c_0, d_0)$$

$$\tau_{gjq}^{-2} \sim \text{Gamma}(e_{0q}, f_{0q})$$

$$\Gamma_j^{-1} \sim \text{Wishart}\{(h_0 \mathbf{H}_{0j})^{-1}, h_0\}$$

where $i = 1, \dots, N$ index subjects, $j = 1, \dots, J$ index groups, and v_g represents the number of voxels in a particular region indexed by $g = 1, \dots, G$ with G as the total region number. We utilized the Desikan-Killiany Atlas regions from FreeSurfer, which included $G = 35$ regions of interest and $\sum_{g=1}^G v_g = 16,384$ voxels in each hemisphere [48]. In the model, $\gamma_{gjq} = (\gamma_{gjq}(1), \dots, \gamma_{gjq}(v_g))$ is the $v_g \times 1$ population-level parameter associated with the q^{th} covariate x_{ijq} , $q = 1, \dots, Q$ where Q is the dimensionality of the covariates of interest. In particular, pairwise spatial correlations among the voxels within the g^{th} region are mediated by the random effect α_{igj} . At the second level, the model expresses a prior belief that each voxel's cortical thickness population mean arises from a normal distribution with a mean given by the overall region mean μ_{0gj} , which is the empirical mean across all subjects and intra-regional voxels, and the variance λ_{gj}^2 . It represents a reasonable starting point to assume that voxels' cortical thickness within anatomically defined regions deviate around an overall mean for that region. Similarly, for each voxel, γ_{gjq} follows a normal distribution with mean γ_{0gjq} and variance τ_{gjq}^2 . At the final level, the hierarchical model captures potential group-related connectivity between brain regions through the covariance matrix Γ_j , which follows the inverse Wishart distribution with the positive definite matrix \mathbf{H}_{0j} as the inverse scale matrix. The Gamma and Wishart distributions are assumed in part due to mathematical/computational convenience. For gamma distribution, we usually set a vague prior (less weight) and have enough data points to estimate the variance well. In case of Wishart distribution, we use the hyper parameter based on the data sample in the same format Kass and Natarajan [49] suggested, with the identity link for the normal distribution. In addition, we also include the covariance structure shrinkage tuning parameter to adjust the strength of belief of between region correlations and implemented in the software [34].

A Markov Chain Monte Carlo (MCMC) method with Gibbs sampling is performed for estimation, and the Gibbs sampling facilitates the estimation by providing substantial reductions in computing time and memory. We set weakly informative priors for the hyperparameters $a_0 = c_0 = e_{0q} = 0.1$, $b_0 = f_{0q} = 0.005$, $d_0 = 0.01$, and $h_0 = G$ (the total number of regions of interest), to ensure that the information in the data primarily governs the results [49]. The selection for h_0 establishes a diffuse prior for the covariance matrix without raising concerns about an improper posterior distribution. More informative priors, however, may be employed when fairly precise information is available. The full conditional distribution for each parameter to run the Gibbs sampler is derived accordingly, which can be referred to Bowman et al. [33]. We performed 10,000 iterations with burn-in of 5,000 iterations and thinning of 10 iterations (for storage and computation time). Despite the apparent complexity and rather rich formulation of our Bayesian hierarchical model as well as the high throughput nature of the data, computations for estimation are quite fast. For

instance, estimation for the Bayesian hierarchical models for our data with 71 PD and 48 controls, the computation time is around one hour with our PC (two duo cores, 16G memory). The region-level parameters and voxel-level parameters showed evidence of convergence, after the burn-in period, in our MCMC analysis. We included age as a covariate in our Bayesian analysis. In preliminary analyses, age showed significant associations with average cortical thickness in each hemisphere with p-values less than 0.01 shown in Fig. 1.

3.2 Neuropsychological Test Analysis

Two sample t-tests were used for group comparisons in demographic information and clinical characteristics (Table 1).

For neuropsychological data, cognitive test scores first were converted to standardized z-scores and then cognitive domains analyzed using analysis of covariance (ANCOVA) with age and HAM-D scores as covariates. All analyses were performed using SAS 9.3 software (SAS Institute, Cary, NC).

3.3 Correlation Analysis between Cortical Thickness and Cognitive Tests

Additional correlation analyses were performed to assess the Spearman's partial correlations between cortical thinning regions within each brain hemisphere and the cognitive variables in both PD patients and Controls. This additional correlation analysis using Spearman's correlation can provide valid measures of their statistical dependence even if non-linear relationship exists.

4 Results

4.1 Demographics

From Table 1, there were no significant differences in age, gender, or education between PDs and Controls due to p-values greater than 0.05. PD patients had significantly higher HAM-D scores ($p < 0.001$) and lower MoCA scores ($p = 0.013$). 21 PD patients had HAM-D scores ≥ 10 , consistent with depressive symptoms [40]. The average disease duration for PD subjects was 4.7 years, with a median of 2.5 years. Average Hoehn and Yahr staging was 1.7, with 28 subjects having stage I disease, 35 subjects having stage II disease, and 8 subjects having stage III disease.

4.2 Cortical Thickness Analysis

The average total left and right cerebral cortical thicknesses for the PD patients were 2.25 ± 0.17 mm and 2.24 ± 0.16 mm, respectively, whereas these of the healthy controls were 2.3 ± 0.11 mm and 2.29 ± 0.11 mm, respectively. As shown in Fig. 1, overall decline of cortical thickness was shown with aging in both Control and PD groups, but this association only achieved statistical significance in the PD group [29].

Fig. 2 shows the cortical thickness differences between PD patients and Controls using the Bayesian hierarchical model with the posterior probability threshold level set at 0.9, i.e. the posterior probability that cortical thickness for PD patients is less than controls,

$\Pr(\text{PD} < \text{Control}) = 0.9$. The thresholded posterior probability maps reveal voxels for which the data provide evidence of cortical thinning in the PD compared with control. PD subjects demonstrated significant cortical thinning in the superior temporal and inferior and superior parietal areas that extended to superior frontal and precuneus regions. Cortical thinning also was found in the left precentral and lateral occipital, and the right postcentral, middle frontal, and fusiform regions. Table 2 gives out the regions information with the posterior probability over 0.9, such as regions' name, coordinates and size.

Considering the potential group-related connectivity between brain regions through the covariance matrix Γ_j , Fig. 3 shows the posterior median of the correlation matrices for both the control and PD in left and right hemisphere. As expected, larger degree of inter-regional connectivity regions were found in superior temporal and inferior and superior parietal to frontal and precuneus regions, to reflect that these affect regions have a stronger inter-regional functional connectivity among the PD group.

4.3 Cognitive Tests

Three PD patients who did not complete parts of the full neuropsychological battery were excluded from this analysis. Table 3 shows that PD subjects performed significantly lower than Controls on tasks related to fine motor speed ($p < 0.001$), processing speed ($p = 0.002$), set-shifting ($p = 0.005$), spontaneous flexibility ($p = 0.02$), and attention ($p = 0.03$). Language, learning/memory, and spatial cognition domains failed to show group differences ($p > 0.05$). Here the raw p -values are obtained based on two-sample t tests and the adjusted p -values are from the multivariate regression models adjusted for age and HAM-D covariates.

4.4 Correlations between Local Cortical Thickness and Cognitive Functions

Spearman's partial correlation analyses with adjustment for age and HAM-D scores were conducted between the brain regions identified in the cortical thickness analysis and cognitive task scores. Table 4 shows that PD patients demonstrated significant positive correlations between the thickness in the fronto-parieto-temporal areas found in the Bayesian model and the executive functions of set shifting and spontaneous flexibility. Controls failed to show any correlations between the thickness and the executive functions ($p > 0.15$).

5 Discussion

In this study, we adopted for the first time a flexible, hierarchical Bayesian spatial model to test the hypothesis that significant cortical thickness changes (i.e., cortical thinning) occur in PD patients without dementia compared with Controls. This model takes advantage of capturing the short-range correlations between voxels within a defined anatomical region as well as the (potentially) long-range inter-regional correlations. The posterior probability inferences were conducted to compute the contrast probability that an affected voxel exceeds some specified threshold (i.e., 0.9), which do not have to consider multiple tests because there are no false positives [33], [50], [51] [52], [53], [54], [55]. Note that we also tried linear mixed-effects models with subject-level and region-level random-effects, but there

were severe convergence issues for the cases with high-dimensionality of regions (i.e., $G=35$). However, the hierarchical Bayesian approach doesn't suffer from this problem and also has the benefit of incorporating a flexible unstructured inter-region correlation matrix and exchangeable intra-region correlations (Fig. 3). Additionally, the Bayesian framework enables us to formulate probabilistic statements that help to quantify the evidence provided by our experimental data. The inference framework also allows us to compute Bayesian credible intervals to make statistical inferences. Further, the MCMC estimation procedures produce samples from the joint posterior distribution of all of the model parameters, which facilitates estimation of and inferences about functions of the model parameters.

We found that PD patients without dementia displayed significant association between the global cortical thinning with aging, with a higher slope than Controls. In addition, the study demonstrated thinning in a number of specific cortical regions in PD, and this localized cortical thinning was significantly correlated with cognitive decline in PD patients. These results support that cortical thinning occurs in PD patients without dementia and may serve as a predictor for cognitive decline in this population.

Previous MR-based cerebral volume studies have revealed GM atrophy and decline of cognitive impairment in PD [11], [12], [13]. VBM analysis of the cerebral cortex, however, can be influenced by GM intensity and cortical folding patterns, and the results of VBM studies in non-demented PD subjects have been variable, and showing regional GM atrophy in frontal, temporal, or parietal cortex [14], [16]. While useful as an exploratory tool, VBM may not be adequate to detect the concrete anatomical changes occurring in the cerebral cortex. The surface-based cortical thickness analysis minimizes the influence of volume-based methods and provides more direct measurements of gray matter changes and insight into disease pathogenesis [26]. Our results show that global cortical thickness decreases with advancing age in PD patients at twice of normal controls (0.47 mm annually vs 0.21 mm, respectively). Using the flexible hierarchical Bayesian spatial model, our study revealed robust cortical thinning findings reported to date in PD subjects without dementia (Fig. 2), and these regions show a higher interregion correlation captured in our model (Fig. 3).

Specifically, our study showed that non-demented PD patients demonstrated widespread cortical thinning in large scale neural networks involving the bilateral inferior and superior parietal regions, including the precuneus, as well as bilateral superior frontal and superior temporal regions compared to Controls. The precuneus has been described as a critical node of information convergence in the parietal network [56]. In addition, PET studies by Eidelberg et al. [9], [57] demonstrated a "PD-related cognitive pattern" (PDCP) that showed reduced metabolism of the dorsolateral premotor cortex (PMC), rostral supplementary motor area (pre-SMA), precuneus, and other posterior parietal regions, and expressed the correlates with performance on neuropsychological tests of memory and executive functioning in non-demented PD patients. Our study for the first time demonstrated a converging pattern of anatomical frontal-parietal-precuneus thinning that occurs in non-demented PD patients and is related to decline in executive cognitive function. Of note, we utilized the Desikan-Killiany atlas regions from FreeSurfer for analysis, which did not separate the SMA and pre-SMA. From our model in Figure 2, (a), (b), the SMA and pre-SMA near precentral and postcentral gyri showed strong posterior related to the frontal-parietal-precuneus regions. In

addition, the thinning in these regions was related to executive cognitive function. These findings support that neuroimaging-based evidence of structural changes may link to PD cortical pathology and the associated cognitive performance.

PET studies have shown that the greatest cerebral glucose metabolic rate reduction in PD occurs in the occipital lobe [58]. Similarly, Nagamachi et al. [59] demonstrated that the greatest difference in hypoperfusion observed between patients with milder PD (H&Y I and II) and patients with advanced PD (H&Y III and IV) was in the occipital cortex. Our findings suggest that left occipital cortex thinning in PD may reflect those functional changes (either as consequences or causes of these changes). Although we do not have visual specific testing or hallucination scores, it is of interest to determine whether the occipital cortical thinning will be predictive of future risk of visual specific dysfunction and/or hallucinations at later stages of the disease [60].

Pathologically PD is associated with a degeneration of the substantia nigra pars compacta of the basal ganglia, but it has been postulated that degeneration extends beyond the basal ganglia and affects more widespread brain areas as disease progresses [8]. It is possible that cortical changes in PD are due to primary cortical GM pathology consisting of Lewy bodies and neurites even in early clinical stage patients [8]. Since many of the cortical areas have direct projections to the striatum, it is also possible that the cortical changes reflect progressive cortico-striatal circuitry dysfunction in PD [3], [13], which may affect the glucose metabolism in cortical regions as shown in PET studies. The chronic “dis-use”, or hypofunction might be underlying the cortical thinning.

As expected, in our study, PD patients without dementia had reduced performance on several neuropsychological tests, particularly involving fine motor speed, processing speed, set-shifting, spontaneous flexibility, and attention (refer to Table 3). Impaired fine motor speed and processing speed may have been exaggerated by testing patients in a practically defined “off” treatment state when there is comparatively greater basal ganglia dysfunction. Executive dysfunction in PD frequently has been attributed to dopamine loss in the striatum that may affect fronto-striatal functions by disrupting activity within cortico-basal ganglia and basal ganglia–thalamocortical circuits [3], [11], [12], [13]. Our MRI cortical thinning analysis, however, also showed that significant morphological brain structural changes occurred in bilateral parietal and superior frontal regions. The current analysis did not reveal group differences in language, spatial cognition, or learning/memory tests. This may be due partly to PD patients in the current study being in early stages of the disease.

We examined the relationship between cortical thinning and cognitive function in PD patients without dementia. The correlations between cortical thinning areas and decline in cognitive domain may extend the understanding of possible pathophysiological substrates underlying PD symptoms. Table 4 shows that moderately strong and statistically significant correlations were found between measures of executive function (including spontaneous flexibility and set-shifting) and cortical thinning in bilateral fronto-parietal regions in the PD sample but not Controls. These regions, including the superior parietal and precuneus, inferior parietal, and superior frontal cortices, have been linked together in a large scale neural network subserving integrative processing for executive functions [54], [56], [61],

[62], [63]. Morphological changes to these regions could contribute to executive function decline separately or in pathophysiologic synergy with basal ganglia dysfunction [64].

In summary, the current results showed that PD patients without dementia sustain cortical thinning which is related to performance reduction in several cognitive domains, with the most robust correlations occurring between fronto-parietal network changes and executive functions.

These results suggest that, in addition to corticostriatal circuit dysfunction, there are cortical anatomical changes and altered functional networks that likely underlie PD cognitive symptoms. Further studies are needed to clarify the effects of disease progression and potentially modifiable neuronal and cognitives.

Acknowledgments

This work was supported by grants National Institutes of Health (NS060722, NS082151, and NS082143), and the HMC GCRC (NIH M01RR10732), GCRC Construction Grant (C06RR016499) and PSU CTSI (TL1 TR000125, Bigdata RFA UL Tr000127). We thank all the participants in the study, as well as their caregivers and the controls.

References

1. Lim SY, Fox SH, Lang AE. Overview of the Extranigral Aspects of Parkinson Disease. *Archives of Neurology*. 2009; 66(2):167–172. [PubMed: 19204152]
2. Kehagia AA, Barker RA, Robbins TW. Neuropsychological and clinical heterogeneity of cognitive impairment and dementia in patients with Parkinson's disease. *Lancet Neurol*. 2010; 9(12):1200–1213. [PubMed: 20880750]
3. Lewis SJ, Dove A, Robbins TW, Barker RA, Owen AM. Cognitive impairments in early Parkinson's disease are accompanied by reductions in activity in frontostriatal neural circuitry. *J Neurosci*. 2003; 23(15):6351–6356. [PubMed: 12867520]
4. Muslimovic D, Post B, Speelman JD, Schmand B. Cognitive profile of patients with newly diagnosed Parkinson disease. *Neurology*. 2005; 65(8):1239–1245. [PubMed: 16247051]
5. Reid W, Hely M, Morris J, Loy C, Halliday G. Dementia in Parkinson's disease: a 20-year neuropsychological study (Sydney Multicentre Study). *Journal of Neurology Neurosurgery and Psychiatry*. 2011; 82(9):1033–1037.
6. Halliday G, Hely M, Reid W, Morris J. The progression of pathology in longitudinally followed patients with Parkinson's disease. *Acta neuropathologica*. 2008; 115(4):409–415. [PubMed: 18231798]
7. Emre M, Aarsland D, Brown R, Burn DJ, Duyckaerts C. Clinical diagnostic criteria for dementia associated with Parkinson's disease. *Mov Disord*. 2007; 22:1689–1707. [PubMed: 17542011]
8. Braak H, Del Tredici K, Rub U, de Vos RA, Jansen Steur EN, Braak E. Staging of brain pathology related to sporadic Parkinson's disease. *Neurobiol Aging*. 2003; 24(2):197–211. [PubMed: 12498954]
9. Eidelberg D. Metabolic brain networks in neurodegenerative disorders: a functional imaging approach. *Trends Neurosci*. 2009; 32(10):548–557. [PubMed: 19765835]
10. Nandhagopal R, McKeown MJ, Stoessl AJ. Functional imaging in Parkinson disease. *Neurology*. 2008; 70(16 Pt 2):1478–1488. [PubMed: 18413571]
11. Ibarretxe-Bilbao N, Junque C, Marti MJ, Tolosa E. Brain structural MRI correlates of cognitive dysfunctions in Parkinson's disease. *J Neurol Sci*. 2011; 310(1–2):70–74. [PubMed: 21864849]
12. Ibarretxe-Bilbao N, Tolosa E, Junque C, Marti MJ. MRI and cognitive impairment in Parkinson's disease. *Mov Disord*. 2009; 24(Suppl 2):S748–753. [PubMed: 19877242]

13. Lee EY, Sen S, Eslinger PJ, Wagner D, Shaffer ML, Kong L, Lewis MM, Du G, Huang X. Early cortical gray matter loss and cognitive correlates in non-demented Parkinson's patients. *Parkinsonism Relat Disord.* 2013; 19(12):1088–93. [PubMed: 23932064]
14. Bruck A, Kurki T, Kaasinen V, Vahlberg T, Rinne JO. Hippocampal and prefrontal atrophy in patients with early non-demented Parkinson's disease is related to cognitive impairment. *Journal of Neurology Neurosurgery and Psychiatry.* 2004; 75(10):1467–1469. doi: DOI: 10.1136/jnnp.2003.031237
15. Camicioli R, Gee M, Bouchard TP, Fisher NJ, Hanstock CC, Emery DJ, Martin WRW. Voxel-based morphometry reveals extra-nigral atrophy patterns associated with dopamine refractory cognitive and motor impairment in parkinsonism. *Parkinsonism Relat Disord.* 2009; 15(3):187–195. [PubMed: 18573676]
16. Nagano-Saito A, Washimi Y, Arahata Y, Kachi T, Lerch JP, Evans AC, Dagher A, Ito K K. Cerebral atrophy and its relation to cognitive impairment in Parkinson disease. *Neurology.* 2005; 64(2):224–229. [PubMed: 15668417]
17. Davatzikos C. Why voxel-based morphometric analysis should be used with great caution when characterizing group differences. *Neuroimage.* 2004; 23(1):17–20. [PubMed: 15325347]
18. Bookstein FL. Voxel-based morphometry should not be used with imperfectly registered images. *Neuroimage.* 2001; 14(6):1454–1462. doi: DOI: 10.1006/nimg.2001.0770 [PubMed: 11707101]
19. Mountcastle VB. The columnar organization of the neocortex. *Brain.* 1997; 120:701–722. [PubMed: 9153131]
20. Du AT, Schuff N, Kramer JH, Rosen HJ, Gorno-Tempini ML, Rankin K, Bruce LM, Weiner MW. Different regional patterns of cortical thinning in Alzheimer's disease and frontotemporal dementia. *Brain.* 2007; 130(Pt 4):1159–1166. [PubMed: 17353226]
21. Kabani N, Le Goualher G, MacDonald D, Evans AC. Measurement of cortical thickness using an automated 3-D algorithm: A validation study. *Neuroimage.* 2001; 13(2):375–380. [PubMed: 11162277]
22. Parent, A., Carpenter, M., editors. *Human neuroanatomy.* Baltimore, MD: Williams & Wilkins; 1995.
23. Rakic P. Specification of Cerebral Cortical Areas. *Science.* 1988; 241(4862):170–176. doi: DOI: 10.1126/science.3291116 [PubMed: 3291116]
24. Jubault T, Gagnon JF, Karama S, Ptito A, Lafontaine AL, Evans AC, Monchi O O. Patterns of cortical thickness and surface area in early Parkinson's disease. *Neuroimage.* 2011; 55(2):462–467. doi: DOI: 10.1016/j.neuroimage.2010.12.043 [PubMed: 21184830]
25. Lyoo CH, Ryu YH, Lee MS. Topographical distribution of cerebral cortical thinning in patients with mild Parkinson's disease without dementia. *Mov Disord.* 2010; 25(4):496–499. [PubMed: 20108369]
26. Zarei M, Ibarretxe-Bilbao N, Compta Y, Hough M, Junque C, Bargallo N, Tolosa E, Marti MJ. Cortical thinning is associated with disease stages and dementia in Parkinson's disease. *J Neurol Neurosurg Psychiatry.* 2013; 84:875–882. [PubMed: 23463873]
27. Pereira JB, Svenningsson P, Weintraub D, Brønneck K, Lebedev A, Westman E, Aarsland D. Initial cognitive decline is associated with cortical thinning in early Parkinson disease. *Neurology.* 2014; 82(22):2017–2025. [PubMed: 24808018]
28. Schill RI, Frost C, Jenkins R, Whitwell JL, Rossor MN, Fox NC. A longitudinal study of brain volume changes in normal aging using serial registered magnetic resonance imaging. *Archives of Neurology.* 2003; 60(7):989–994. [PubMed: 12873856]
29. Salat DH, Buckner RL, Snyder AZ, Greve DN, Desikan RS, Busa E, Morris JC, Dale AM, Fischl B. Thinning of the cerebral cortex in aging. *Cereb. Cortex.* 2004; 14:721–730. [PubMed: 15054051]
30. Pagonabarraga J, Corcuera-Solano I, Vives-Gilabert Y, Llebaria G, García-Sánchez C, Pascual-Sedano B, Delfino M, Kulisevsky J, Gómez-Ansón B. Pattern of Regional Cortical Thinning Associated with Cognitive Deterioration in Parkinson's Disease. *PLoS ONE.* 2013; 8(1):e54980. [PubMed: 23359616]
31. Pereira JB, Ibarretxe-Bilbao N, Marti MJ, Compta Y, Junque C, Bargallo N, Tolosa E. Assessment of cortical degeneration in patients with Parkinson's disease by voxel-based morphometry, cortical

- folding, and cortical thickness. *Hum Brain Mapp.* 2012; 33(11):2521–2534. doi: DOI: 10.1002/hbm.21378 [PubMed: 21898679]
32. Segura B, Baggio HC, Marti MJ, Valldeoriola F, Compta Y, Garcia-Diaz AI, Vendrell P, Bargallo N, Tolosa E, Junque EC. Cortical thinning associated with mild cognitive impairment in Parkinson's disease. *Mov. Disord.* 2014; 29:1495–1503. doi: DOI: 10.1002/mds.25982 [PubMed: 25100674]
 33. Bowman FD, Caffo B, Bassett SS, Kilts C. A Bayesian hierarchical framework for spatial modeling of fMRI data. *Neuroimage.* 2008; 39(1):146–156. [PubMed: 17936016]
 34. Zhang L, Agravat S, Derado G, Chen S, McIntosh BJ, Bowman FD. BSMac: A MATLAB toolbox implementing a Bayesian spatial model for brain activation and connectivity. *Journal of Neuroscience Methods.* 2012; 204(1):133–143. [PubMed: 22101143]
 35. Calne DB, Snow BJ, Lee C. Criteria for Diagnosing Parkinsons-Disease. *Annals of Neurology.* 1992; 32:S125–S127. [PubMed: 1510370]
 36. Jurica, P., Leitten, C., Mattis, S. *Dementia Ratings Scale-2: Professional Manual.* Odessa FL: Psychological Assessment Resources; 2001.
 37. Dubois B, Burn D, Goetz C, Aarsland D, Brown RG, Broe GA, Dickson D, Duyckaerts C, Cummings J, Gauthier S, Korczyn A, Lees A, Levy R, Litvan I, Mizuno Y, McKeith IG, Olanow CW, Poewe W, Sampaio C, Tolosa E, Emre M. Diagnostic procedures for Parkinson's disease dementia: recommendations from the Movement Disorder Society Task Force. *Mov Disord.* 2007; 22(16):2314–2324. [PubMed: 18098298]
 38. Langston JW. Neurotoxins and Their Potential Roles in Neurodegeneration Held by the New-York-Academy-of-Sciences on May 6–8, 1991 in New York, New-York – Preface. *Annals of the New York Academy of Sciences.* 1992; 648:R11–R13.
 39. Hoehn MM, Yahr MD. Parkinsonism - Onset Progression and Mortality. *Neurology.* 1967; 17(5): 427–442. [PubMed: 6067254]
 40. Hamilton M. A Rating Scale for Depression. *Journal of Neurology Neurosurgery and Psychiatry.* 1960; 23(1):56–62.
 41. Hachinski V, Iadecola C, Petersen RC, Breteler MM, Nyenhuis DL, Black SE, Powers WJ, DeCarli C, Merino JG, Kalra RN, Vinters HV, Holtzman DM, Rosenberg GA, Wallin A, Dichgans M, Marler JR, Leblanc GG. National Institute of Neurological Disorders and Stroke-Canadian Stroke Network vascular cognitive impairment harmonization standards. *Stroke.* 2006; 37(9):2220–41. [PubMed: 16917086]
 42. Segonne F, Dale AM, Busa E, Glessner M, Salat D, Hahn HK, Fischl B. A hybrid approach to the skull stripping problem in MRI. *Neuroimage.* 2004; 22(3):1060–1075. [PubMed: 15219578]
 43. Fischl B, Salat DH, van der Kouwe AJW, Makris N, Segonne F, Quinn BT, Dale AM. Sequence-independent segmentation of magnetic resonance images. *Neuroimage.* 2004; 23:S69–S84. [PubMed: 15501102]
 44. Sled JG, Zijdenbos AP, Evans AC. A nonparametric method for automatic correction of intensity nonuniformity in MRI data. *IEEE Trans. on Medical Imaging.* 1998; 17(1):87–97. [PubMed: 9617910]
 45. Segonne F, Pacheco J, Fischl B. Geometrically accurate topology-correction of cortical surfaces using nonseparating loops. *IEEE Trans. on Medical Imaging.* 2007; 26(4):518–529. [PubMed: 17427739]
 46. Dale AM, Fischl B, Sereno MI. Cortical surface-based analysis - I. Segmentation and surface reconstruction. *Neuroimage.* 1999; 9(2):179–194. doi: DOI: 10.1006/nimg.1998.0395 [PubMed: 9931268]
 47. Fischl B, Dale AM. Measuring the thickness of the human cerebral cortex from magnetic resonance images. *Proc Natl Acad Sci USA.* 2000; 97(20):11050–11055. [PubMed: 10984517]
 48. Desikan RS, Segonne F, Fischl B, Quinn BT, Dickerson BC, Blacker D, Buckner RL, Dale AM, Maguire RP, Hyman BT, Albert MS, Killiany RJ. An automated labeling system for subdividing the human cerebral cortex on MRI scans into gyral based regions of interest. *Neuroimage.* 2006; 31(3):968–80. [PubMed: 16530430]
 49. Kass RE, Natarajan R. A default conjugate prior for variance components in generalized linear mixed models (comment on article by Browne and Draper). *Bayesian Analysis.* 2006; 1:535–542.

50. Friston KJ, Glaser DE, Henson RNA, Kiebel S, Phillips C, Ashburner J. Classical and Bayesian inference in neuroimaging: applications. *NeuroImage*. 2002; 16:484–512. [PubMed: 12030833]
51. Friston KJ, Penny W, Phillips C, Kiebel S, Hinton G, Ashburner J. Classical and Bayesian inference in neuroimaging: theory. *NeuroImage*. 2002; 16:465–483. [PubMed: 12030832]
52. Friston KJ, Penny W. Posterior probability maps and SPMs. *NeuroImage*. 2003; 19:1240–1249. [PubMed: 12880849]
53. Berry DA, Hochberg Y. Bayesian perspectives on multiple comparisons. *J. Stat. Plan. Infer.* 1999; 82:215–227.
54. Tadesse M, Ibrahim J, Vannucci M, Gentleman R. Wavelet thresholding with Bayesian false discovery rate control. *Biometrics*. 2005; 61(1):25–35. [PubMed: 15737075]
55. Blume JD. Tutorial in biostatistics: likelihood methods for measuring statistical evidence. *Stat. Med.* 2002; 21:2563–2599. [PubMed: 12205699]
56. Cavanna AE, Trimble MR. The precuneus: a review of its functional anatomy and behavioural correlates. *Brain*. 2006; 129:564–583. doi: DOI: 10.1093/Brain/Awl004 [PubMed: 16399806]
57. Fitzpatrick T, Mattis P, Eidelberg D D. Functional Imaging of Cognitive Impairment in Parkinson's Disease. *Clinical Eeg and Neuroscience*. 2010; 41(3):119–126. [PubMed: 20722344]
58. Bohnen NI, Minoshima S, Giordani B, Frey KA, Kuhl DE. Motor correlates of occipital glucose hypometabolism in Parkinson's disease without dementia. *Neurology*. 1999; 52(3):541–546. [PubMed: 10025784]
59. Nagamachi S, Wakamatsu H, Kiyohara S, Fujita S, Futami S, Tamura S, Nakazato M, Yamashita S, Arita H, Nishii R, Kawai K. Usefulness of rCBF analysis in diagnosing Parkinson's disease: supplemental role with MIBG myocardial scintigraphy. *Annals of Nuclear Medicine*. 2008; 22(7): 557–564. [PubMed: 18756357]
60. Ramirez-Ruiz B, Marti MJ, Tolosa E, Gimenez M, Bargallo N, Valldeoriola F, Junque C. Cerebral atrophy in Parkinson's disease patients with visual hallucinations. *European Journal of Neurology*. 2007; 14(7):750–756. [PubMed: 17594330]
61. Newman SD, Carpenter PA, Varma S, Just MA. Frontal and parietal participation in problem solving in the Tower of London: fMRI and computational modeling of planning and high-level perception. *Neuropsychologia*. 2003; 41(12):1668–82. [PubMed: 12887991]
62. Naghavi HR, Nyberg L. Common fronto-parietal activity in attention, memory, and consciousness: shared demands on integration? *Conscious Cogn.* 2005; 14(2):390–425. [PubMed: 15950889]
63. Vincent JL, Kahn I, Snyder AZ, Raichle ME, Buckner RL. Evidence for a Frontoparietal Control System Revealed by Intrinsic Functional Connectivity. *J Neurophysiol.* 2008; 100(6):3328–3342. [PubMed: 18799601]
64. Monchi O, Petrides M, Doyon J, Postuma RB, Worsley K, Dagher A. Neural bases of set-shifting deficits in Parkinson's disease. *Journal of Neuroscience*. 2004; 24(3):702–710. [PubMed: 14736856]

Biographies



Lijun Zhang is an Assistant Professor in the Institute for Personalized Medicine at Penn State University, College of Medicine. He received his Ph.D in Computer Science from Univ. of Louisville, KY, and had his postdoc training both in the Dept of Biostatistics and Bioinformatics at Emory University, and the Dept. of Neurology at PSU. Dr. Zhang's

research focuses on statistical methods on high dimensional neuroimaging and genomics data, and machine learning with pattern recognition and image processing.



Ming Wang is an assistant professor in the Division of Biostatistics and Bioinformatics, Department of Public Health at Penn State Hershey Medical Center. She obtained a Ph.D degree in Biostatistics from Emory University in 2013. Her research interest spans several topics including spatial-temporal analysis, longitudinal data analysis, survival analysis and clinical trials with respect to prostate cancer, acute kidney injury and Parkinson's disease.



Young Truong is professor in the Dept of Biostatistics at the University of North Carolina at Chapel Hill. Dr. Truong has Ph.D in Statistics from University of California, Berkeley. His research includes time series, independent component analysis, neuroimaging modeling, and Biochemical Epidemiology.



F. Dubois Bowman is the chair of the Dept. of Biostatistics at the Mailman School of Public Health and professor of Biostatistics at Columbia University. Dr. Bowman obtained his PhD in Biostatistics from the University of North Carolina, Chapel Hill. He founded and served as director of the Center for Biomedical Imaging Statistics at Emory Univ. Dr. Bowman leads an active statistical research program focusing on mental health disorders such as major depression as well as neurological disorders such as PD. His research encompasses multiple imaging modalities, including fMRI, DTI, and PET.



Xuemei Huang is a professor in the Dept. of Neurology, Neurosurgery, Radiology, Pharmacology and Kinesiology, at Penn State University and Penn State Hershey Medical Center. She is the Vice Chair for Research in the Dept. of Neurology, PSU-Hershey, and Director of Hershey Brain Analysis Research Laboratory for Neurodegenerative Disorders. Dr. Huang is a board-certified research neurologist and movement disorder specialist whose clinical practice and scholarly interests are focused on neurodegenerative disorders, particularly on PD. One of her research focuses is on the use of novel imaging modalities and designs to elucidate neurocircuitry underlying various signs and symptoms of PD, and the development of imaging biomarkers for early detection and progression of PD.

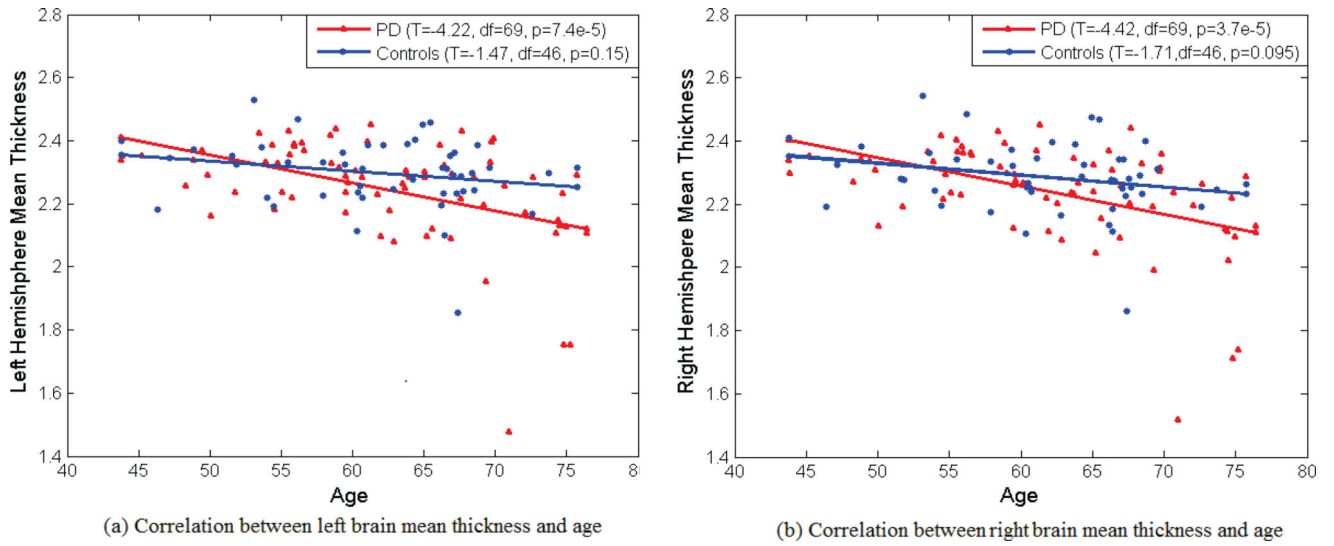


Fig. 1. Correlation between brain mean thickness and age in PD and Controls. Each hemisphere data are plotted separately: (a) left hemisphere, (b) right hemisphere.

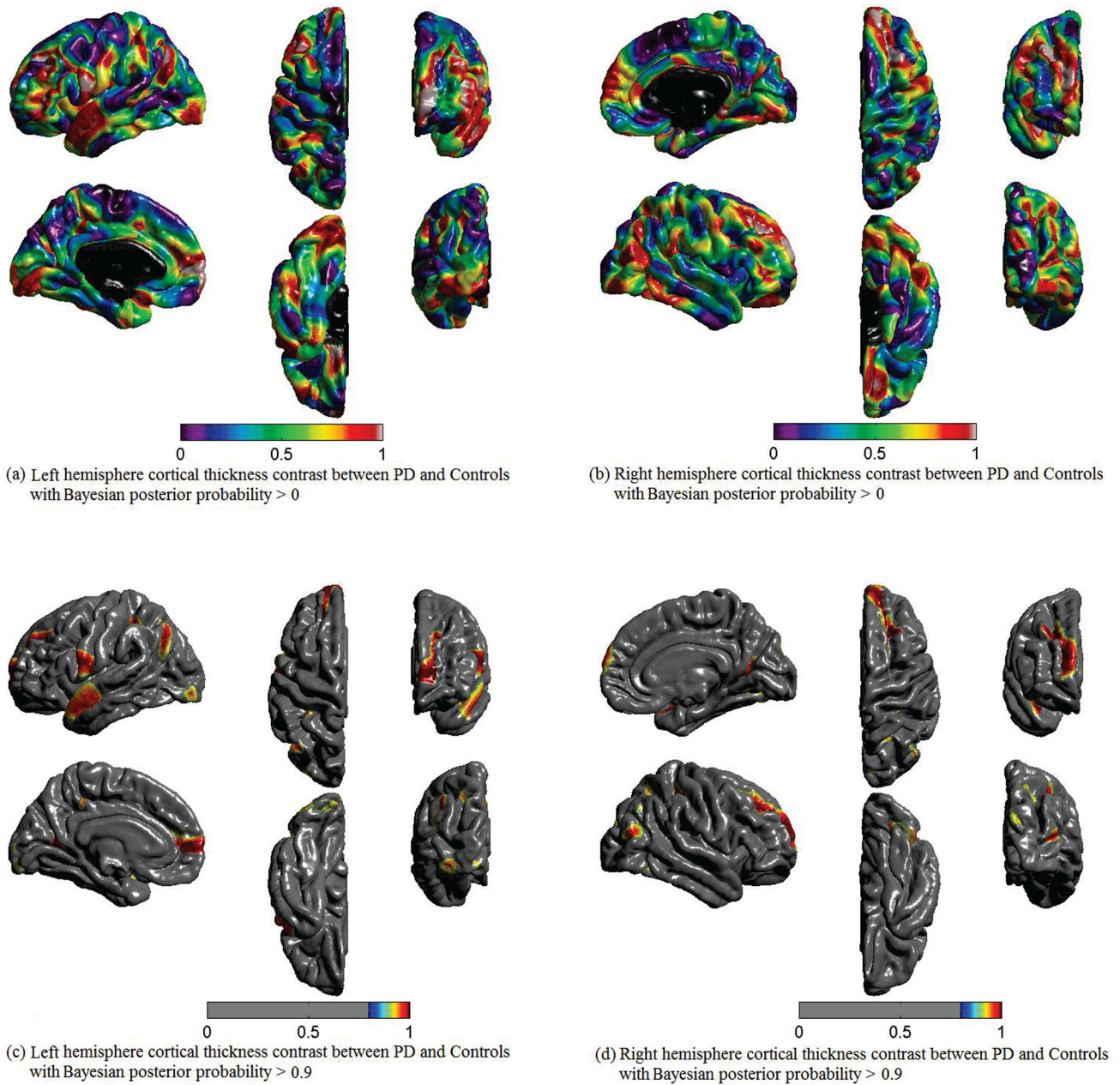


Fig. 2. Cortical thickness contrast between PD and Controls using Bayesian hierarchical model. $\Pr(\text{PD} < \text{Controls})$. (a) Left hemisphere with the posterior probability that the cortical thickness for PD is less than Controls, threshold level set at 0, i.e. $\Pr(\text{PD} < \text{Control}) > 0$; (b) Right hemisphere with the posterior probability threshold level set at 0; (c) Left hemisphere with the posterior probability threshold level set at 0.9, i.e. $\Pr(\text{PD} < \text{Control}) > 0.9$; (d) Right hemisphere with the posterior probability threshold level set at 0.9.

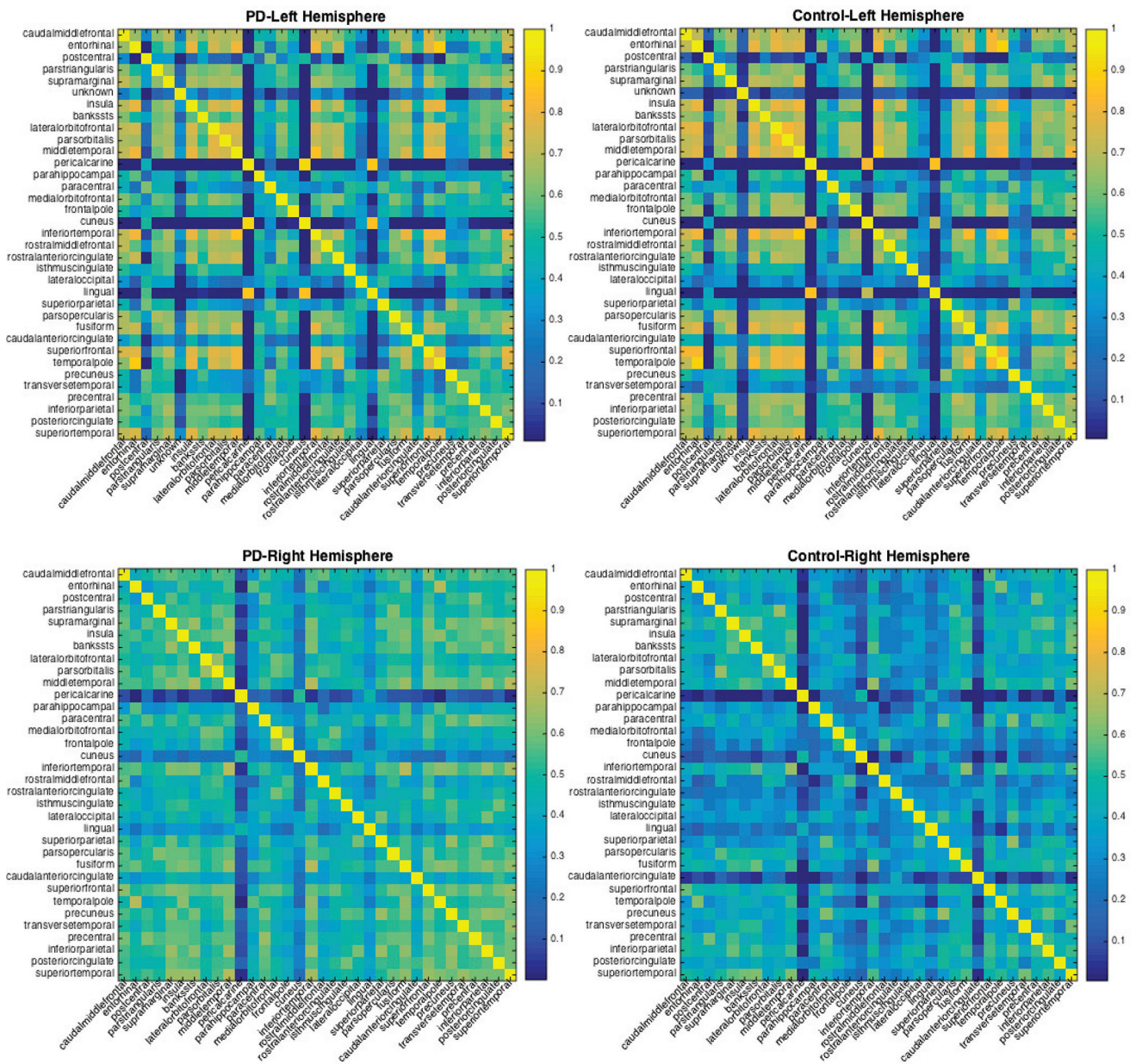


Fig. 3. Posterior median correlation estimates of inter-regional connectivity for the PD data set. Top row are median correlation matrices for both the PD and Controls in the left hemisphere, bottom row show median correlation for PD and Control in the right hemisphere.

TABLE 1

subjects' Demographic information in the study

Measure	Controls (n=48)	PDs (n=71)	p-value
Age (years)	61.70±7.35	62.21±8.59	0.73
Education (years)	15.78±2.89	14.97±2.73	0.13
Gender, M:F	30:18	40:28	0.69
Duration of disease (years)	NA	4.7±5.3	NA
UPDRS	NA	21.4±11.8	NA
HAM-D	3.71±2.34	7.17±4.12	<0.001
MoCA	26.15±2.24	24.75±3.67	0.013

Note: Mean±Standard Deviation (SD) for continuous variables, and frequencies for categorical variables. The p-values are based on two-sample t-tests for continuous variables and Pearson's Chi-square tests for categorical variables. The significance level was 0.05. (NA = not applicable).

Table 2

Regions having posterior probability > 0.9

	X	Y	Z	Region Size (voxel #)
Left Hemi- Cortical Name				
Lateral occipital	-21	-91	-13	673
Superior parietal	-34	-48	44	1192
Superior frontal	-9	45	16	2154
Precuneus	-17	-60	17	857
Precentral	-50	5	18	1868
Inferior parietal	-42	-69	33	873
Superior temporal	-54	1	-20	1694
Right Hemi-Cortical Name				
Postcentral	36	-36	50	689
Rostral middle frontal	28	33	38	684
Superior parietal	24	-63	44	703
Fusiform	42	-63	-13	775
Superior frontal	20	43	35	2129
Precuneus	21	-62	12	710
Inferior parietal	45	-72	19	676
Superior temporal	44	1	-19	857

Author Manuscript

Author Manuscript

Author Manuscript

Author Manuscript

Table 3

Neuropsychological test results for control and PD subjects.

Test	Controls (n =48)	PD (n =68)	Raw p- value ^a	Adjusted p-value ^b
Fine motor speed				
<i>Mean z-score</i>	-0.48 ± 1.44	-3.66 ± 3.53	< 0.001	< 0.001
GPD_D	-0.50 ± 1.47	-4.13 ± 4.99	< 0.001	< 0.001
GPD_ND	-0.46 ± 1.62	-3.19 ± 3.24	< 0.001	< 0.001
Processing speed				
<i>Mean z-score</i>	0.62 ± 0.66	0.27 ± 0.89	0.01	0.002
CWInt Color	0.54 ± 0.76	0.22 ± 0.99	0.06	0.008
Symbol Search	0.71 ± 0.87	0.37 ± 0.95	0.05	0.002
Executive function: Set-shifting				
<i>Mean z-score</i>	0.31 ± 0.42	-0.17 ± 0.98	0.0004	0.005
CWInt Inhibition	0.55 ± 0.65	0.08 ± 1.25	0.01	0.03
CWInt Inhibition Errors	0.32 ± 0.59	-0.44 ± 1.24	< 0.001	0.81
CWInt Switch	0.49 ± 0.97	0.30 ± 1.11	0.33	0.03
CWInt Switch Errors	0.49 ± 0.61	0.01 ± 1.03	0.002	0.70
VVT Total	0.09 ± 0.87	-0.27 ± 1.37	0.09	0.0002
VVT Switch	-0.07 ± 0.88	-0.55 ± 1.44	0.03	0.0006
Executive function: Spontaneous flexibility				
<i>Mean z-score</i>	0.29 ± 0.55	-0.02 ± 0.77	0.01	0.02
DesFlu Switch	0.69 ± 0.82	0.25 ± 1.09	0.02	0.04
DesFlu Total Correct	0.65 ± 0.97	0.19 ± 1.09	0.02	0.04
DesFlu Total Design	0.99 ± 1.19	0.59 ± 1.52	0.13	0.17
DesFlu Design Accuracy	-0.56 ± 0.98	-0.77 ± 1.20	0.33	0.34
VerbFlu Letter	-0.08 ± 0.87	-0.26 ± 1.15	0.34	0.14
VerbFlu Category	0.03 ± 0.93	-0.14 ± 1.08	0.37	0.18
Language				
<i>Mean z-score</i>	0.46 ± 0.58	0.32 ± 0.75	0.29	0.25
CWInt Word	0.48 ± 0.71	0.31 ± 1.06	0.30	0.27
BNT	0.44 ± 0.93	0.33 ± 1.05	0.57	0.60
Spatial cognition				
<i>Mean z-score</i>	-0.09 ± 0.69	-0.33 ± 0.96	0.13	0.18
JoLO	-0.19 ± 1.37	-0.49 ± 1.79	0.32	0.32
DRS2 Construction	0	-0.14 ± 0.40	0.005	0.06
Memory				
<i>Mean z-score</i>	-0.42 ± 0.91	-0.72 ± 1.07	0.12	0.13
BVMT-R Total Learning	-0.34 ± 1.29	-0.72 ± 1.33	0.13	0.18
BVMT-R Delayed Recall	0.03 ± 1.41	-0.44 ± 1.36	0.11	0.22

Test	Controls (n =48)	PD (n =68)	Raw p- value ^a	Adjusted p-value ^b
BVMT-R Discrimination Index*	-0.69 ± 1.98	-1.27 ± 2.51	0.19	0.39
HVLT-R Total Learning	-0.53 ± 0.89	-0.69 ± 0.97	0.36	0.09
HVLT-R Delayed Recall	-0.70 ± 1.05	-0.64 ± 1.09	0.76	0.93
HVLT-R Discrimination Index*	-0.30 ± 1.04	-0.53 ± 1.15	0.28	0.11
Attention				
<i>Mean z-score</i>	0.46 ± 0.48	0.17 ± 0.72	0.01	0.03
Letter Number Sequencing	0.35 ± 0.58	0.13 ± 0.95	0.13	0.16
Spatial Span	0.52 ± 0.85	0.28 ± 1.05	0.20	0.26
Digit Span	0.52 ± 0.71	0.10 ± 0.76	0.003	0.008

Note: Mean±Standard Deviation (SD) is shown for all continuous variables.

Mean z-score: The average z-score from all sub-categories.

^a: The p-value is obtained based on a two-sample t-test for each variable.

^b: The adjusted p-value is obtained based on the multivariate regression models adjusting for age and HAMD covariates.

Note: Neuropsychological test results showing Mean ± Standard Deviation (SD). All test scores were converted to standard z-scores. Higher z-scores

Table 4

Spearman correlation (r) and p -value (p) between cognitive domain test and localized thinning regions for PD and control

Region Name	PD		Control	
	Set-shifting	Spontaneous Flexibility	Set-shifting	Spontaneous Flexibility
Left Cortical Region				
Lateral occipital	$r=0.28$ ($p=0.025$)	0.26 (0.036)	0.15 (0.32)	0.15 (0.31)
Superior parietal	$r=0.27$ ($p=0.027$)	0.29 (0.019)	0.21 (0.15)	0.10 (0.49)
Superior frontal	$r=0.31$ ($p=0.012$)	0.29 (0.019)	0.14 (0.36)	0.13 (0.38)
precuneus	$r=0.27$ ($p=0.028$)	0.25 (0.041)	0.13 (0.4)	0.11 (0.48)
precentral	$r=0.28$ ($p=0.025$)	0.27 (0.029)	0.14 (0.35)	0.14 (0.34)
Inferior parietal	$r=0.27$ ($p=0.03$)	0.26 (0.034)	0.13 (0.39)	0.12 (0.41)
Superior temporal	$r=0.26$ ($p=0.039$)	0.26 (0.035)	0.14 (0.35)	0.14 (0.36)
Right Cortical Region				
postcentral	$r=0.24$ ($p=0.051$)	0.24 (0.05)	0.13 (0.37)	0.15 (0.33)
Rostral middle frontal	$r=0.31$ ($p=0.012$)	0.31 (0.011)	0.10 (0.50)	0.14 (0.36)
Superior parietal	$r=0.33$ ($p=0.006$)	0.34 (0.006)	0.11 (0.46)	0.15 (0.30)
fusiform	$r=0.26$ ($p=0.035$)	0.27 (0.029)	0.09 (0.51)	0.13 (0.36)
Superior frontal	$r=0.28$ ($p=0.026$)	0.29 (0.017)	0.10 (0.48)	0.14 (0.35)
precuneus	$r=0.30$ ($p=0.016$)	0.32 (0.009)	0.09 (0.51)	0.17 (0.25)
Inferior parietal	$r=0.32$ ($p=0.010$)	0.32 (0.01)	0.08 (0.60)	0.15 (0.30)
Superior temporal	$r=0.35$ ($p=0.005$)	0.32 (0.01)	0.10 (0.50)	0.19 (0.21)